Marine aerosol properties over the Southern Ocean in relation to the wintertime meteorological conditions

Manu Anna Thomas[1], Abhay Devasthale[1], and Michael Kahnert[1,2]

[1]Swedish Meteorological and Hydrological Institute, Folkborgsvägen 17, 60176 Norrköping, Sweden.
[2]Chalmers University of Technology, Chalmersplatsen 4, 41296 Gothenburg, Sweden.

Correspondence: Manu Anna Thomas (manu.thomas@smhi.se)

Abstract.

Given the vast expanse of oceans on our planet, marine aerosols, and sea salt in particular, play an important role in the climate system via multitude of direct and indirect effects. The efficacy of their net impact however depends strongly on the local meteorological conditions that influence their physical, optical and chemical properties. Understanding the coupling between aerosol properties and meteorological conditions is therefore important. It has been historically difficult to statistically quantify this coupling over larger oceanic areas due to the lack of suitable observations, leading to large uncertainties in the representation of aerosol processes in climate models. Perhaps no other region shows higher uncertainties in the representation of marine aerosols and their effects than the Southern Ocean. During winter the Southern Ocean boundary layer is dominated by sea salt emissions.

Here, using 10 years of austral winter period (June, July and August, 2007-2016) space based aerosol profiling by CALIOP-CALIPSO in combination with meteorological reanalysis data, we investigated the sensitivity of marine aerosol properties over the Southern Ocean (40S-65S) to various meteorological parameters, such as vertical relative humidity (RH), surface wind speed, and sea surface temperature (SST) in terms of joint histograms. The sensitivity study is done for the climatological conditions as well as for the enhanced cyclonic and anticyclonic conditions in order to understand the impact of large-scale atmospheric circulation on the aerosol properties.

We find a clear demarcation in the 532 nm aerosol backscatter and extinction at RH around 60%, irrespective of the state of the atmosphere. The backscatter and extinction increase at higher relative humidity as a function of surface wind speed. This is mainly because of the water uptake by the wind driven sea salt aerosols at high RH near the ocean surface resulting in an increase in size, which is confirmed by the decreased depolarization for the wet aerosols. An increase in aerosol backscatter and extinction is observed during the anticyclonic conditions compared to cyclonic conditions for the higher wind speeds and relative humidity, mainly due to aerosols being confined to the boundary layer and their proximity to the ocean surface facilitates the growth of the particles. We further find a very weak dependency of aerosol backscatter on SSTs at lower wind speeds. But when the winds are stronger than about 12 m/s, the backscattering coefficient generally increases with SST.

When aerosol properties are investigated in terms of aerosol verticality and in relation to meteorological parameters, it is seen that the aerosol backscatter values in the free troposphere (pressure < 850 hPa) are much lower than in the boundary layer, irrespective of the RH and the three weather states. This indicates that the local emissions from the ocean surface make the

dominant contribution to aerosol loads over the Southern Ocean. A clear separation of particulate depolarization is observed in the free and lower troposphere, more prominent in the climatological mean and the cyclonic states. For RH > 60%, low depolarization values are noticeable in the lower troposphere, which is an indication of the dominance of water-coated, mostly
30 spherical sea salt particles. For RH < 60%, there are instances when the aerosol depolarization increases in the boundary layer, more prominently in the mean and anticyclonic cases which can be associated with the presence of drier aerosol particles.

We also note some limitations of our study. For example, interpreting the verticality of aerosol properties (especially depolarization) in relation to the meteorological conditions in the free and upper troposphere (pressure < 850 hPa) was challenging. Furthermore, we do not see any direct evidence of sudden crystallization (efflorescence), deliquescence, or hysteresis effects of
35 the aerosols. Observing such effects will likely require a targeted investigation of individual cases considering tracer transport, rather than the statistical sensitivity study that entails temporally and geographically averaged large data sets.

1   Introduction

Aerosols, irrespective of their phase, are defined as particles, suspended in the air with lifetimes ranging from hours to decades. Atmospheric aerosols, both natural and anthropogenic, present themselves in multitude of sizes, shapes and chemical com-
40 position. Oceanic sea salt and biogenic emissions, desert dust and volcanic emissions constitute natural sources of aerosols. All others that are as a result of human interference, directly or indirectly such as industrialization, agriculture and forest fires are classified as aerosols derived from anthropogenic sources. Aerosols are very complex in nature and influence the Earth system through their impact on climate, environment and health. Aerosol research focusing on the nature of aerosols and their interactions has progressed significantly over the last decade, given their implications for the Earth's radiative balance. The
45 IPCC AR5 reports the global mean direct aerosol radiative forcing is -0.35 W/m^2, with a range of –0.85 to +0.15 W/m^2. The radiative forcing estimates due to the aerosol-cloud interactions, the so-called indirect effects, are still investigatory with a best estimate value of -0.9 W/m^2.

Among the naturally occurring aerosols, oceans are the dominant source of such aerosols in the form of sea salt with total emission ranging from 1,400 to 6,800 Tg/yr according to the IPCC Fifth Assessment Report (2013). Sea salt aerosols are highly
50 hygroscopic in nature and play an important role in the chemistry of the marine atmosphere (Weng et al., 2020). As they are an important source of halogens, they are capable of altering the chemistry of several species such as ozone, nitrogen, bromine etc via heterogeneous reactions (Sievering et al., 1992; Vogt et al., 1999; Zhu et al., 2019). The dependency of the hygroscopicity of sea salt aerosols on the ambient humidity means that they can impact the amount of radiation that is attenuated thereby affecting the clear sky radiative fluxes (Haywood et al., 1999; Ma et al., 2008). Also, they are very efficient CCN thereby altering the
55 cloud albedo, lifetime and eventually precipitation (Kaufman et al., 2001; Shinozuka et al., 2004; Pierce and Adams, 2006).

Pure sea salt contains 85% salt. Mostly it consists primarily of NaCl and a mixture of one or more of other salts, such as, Mg, K, Ca sulfates etc and traces of organic material. Since sea salt is highly hygroscopic, the ambient relative humidity (RH) determines their morphology and refractive index (Tang, 1997; Irshad et al., 2009; Cotterell et al., 2017). In marine environments, RH can reach as high as 80-90%. Deliquescence and efflorescence phase transformations of sea salt are more

60   complex and depend on the RH values and the composition. As the RH increases, deliquescence occurs at about 76% RH

which is termed as deliquescence RH (DRH). However, as RH decreases, the moist particle does not crystallize at DRH, but at

a much lower RH (values below 45%) (Wise et al., 2009). This hysteresis effect has been studied in detail in the laboratory for

different salts (Tang, 1996, 1997). Hygroscopic growth of inorganic sea salt is 8-15% lower than that of NaCl (Zeng et al., 2013;

Zieger et al., 2017). Sea salt particles come in a range of sizes with dry sea salt aerosols being relatively smaller than those at

65   high RH (Lewis and Schwartz, 2004; Zhang et al., 2005). The influence of RH on aerosol light scattering is evaluated by the

scattering enhancement factor which varies considerably depending on the size and type of aerosol and their transport pathway

(Zieger et al., 2013). The cloud radar at the Barbados Cloud Observatory which is situated at the windward coast of Barbados

(13.16°N, 59.43°W) is found to be well-suited as the propagation of the ITCZ to the SH during NH winter favors the transport

of dust-laden air masses to South America leaving this station solely under marine influence (Stevens et al., 2016). This is an

70   ideal condition to explore the sea salt aerosols in detail in their natural environment. Haarig et al. (2017) studied the linear

depolarization ratios over Barbados and observed that there were periods with RH below 40% for which the depolarization

ratios significantly increased to 0.15 ± 0.03 (at 532 nm) compared to the laboratory measurement values of 0.08±0.01 for

sea-salt crystals (Sakai et al., 2010). This implies that the naturally occurring sea salt particles are not completely dry, but are

starting to crystallize. This can have an impact on the Earth's radiative budget.

75   Apart from the laboratory studies and in-situ observations, numerous campaigns have been carried out to assess the size,

morphology and the composition of naturally occurring sea salt (For example: ATom (Atmospheric Tomography mission)

aircraft campaign (Froyd et al., 2019; Murphy et al., 2019); The ACE1 (First Aerosol Characterization Experiment) flight

campaigns (Bates et al., 1998a); PEMT-B (Pacific Exploratory Mission in the tropics) flight campaign (Fuelberg et al., 2001)

etc). All these campaigns were aimed at understanding the physical, chemical and optical properties of tropospheric marine

80   aerosols under clean atmospheric conditions and their dependency on different synoptic states. It was observed that 26% of the

accumulation mode particles below 200 m was sea salt and this fraction increases with wind speed. The scattering coefficients

of sea salt decreases to 87% under dry conditions compared to 96% at high relative humidities and sea salt contributes to about

63% of the total column AOD (aerosol optical depth) over the Southern Oceans (Shinozuka et al., 2004).

Being one of the dominant aerosol types in the atmosphere and the impact they can instil on the Earth's radiative balance,

85   the role of the sea salt aerosols in the climate system can not be ignored. At the same time, due to their complex nature and

high computational costs, the atmospheric flux of sea salt in the general circulation models is heavily parameterized based

on existing campaign measurements. There are two main ways by which sea salt is released into the atmosphere; one by the

bursting of air bubbles during whitecap formation and other by the direct tearing of droplets from the top of breaking waves.

These two processes release sea salt droplets of varying radii with smaller droplets of size range 0.25 – 8 μm by the former

90   mechanism and much larger droplets (10- 20 μm) by the latter (Guelle et al., 2001; de Leeuw et al., 2000). The generation of

sea spray in the models are described by source functions that are factors of surface wind speed and/or water temperature and

are based on field and/or laboratory data (e.g. Smith et al. (1993); O'Dowd et al. (1997); Andreas (1998); Smith et al. (1993);

Vignati et al. (2001); de Leeuw et al. (2000); Monahan et al. (1986); Martensson et al. (2003); Gong (2003)). Clarke et al.

(2006) considered ultrafine sea salt as they can have an impact on the CCN concentrations. However, a detailed review of these

95   source functions revealed that the sea spray fluxes varied by several orders of magnitude for different size ranges and wind
speeds (Guelle et al., 2001; Vignati et al., 2001; Gong, 2003; Lewis and Schwartz, 2004). All these and many more of these
parameterizations were evaluated extensively in the general circulation models (Tsyro et al., 2011; Spada et al., 2015; Neumann
et al., 2016; Revell et al., 2019; Weng et al., 2020). It was seen that the atmospheric sea salt concentrations were overestimated
by 8 - 46% and the concentrations in precipitation were systematically underestimated by nearly 70% over Europe and can
100   be attributed to the sensitivity to the meteorology used and also uncertainties in the processes such as deposition velocities,
in-cloud scavenging ratio etc (Tsyro et al., 2011). Jaeglé et al. (2011) obtained model bias reductions of nearly a factor of two
for both cruise and station observations globally when an empirical source function depending on both wind speed and sea
surface temperature was used. A recent work by Grythe et al. (2014) suggested a new source function with an averaged wind
speed dependency of $u_{10}^{3.5}$ and temperature produced sea salt spray emissions close to the observations. Many of these studies
105   failed to accurately reproduce the aerosol optical depth. For example, the ACCMIP (Atmospheric Chemistry and Climate
Model Intercomparison Project) models and other studies overestimated the winter AOD over the Southern Oceans because of
the overestimation of the wind speed dependency introduced by the sea spray source function used in the model (Jaeglé et al.,
2011; Shindell et al., 2013; Spada et al., 2015; Revell et al., 2019).

Given their dominance in the atmosphere, multitude of climate impacts, their sensitivity to the local meteorology and their
110   poor representation in global climate models, it is important to continue to study and characterize sea-salt aerosols under
varying meteorological conditions. The oceanic area covers approximately 70% of the Earth's surface and since the majority
of these water bodies are bounded by continents, it makes it difficult to separate the naturally occurring sea salt aerosols
from other natural/anthropogenic aerosols in order to study the characteristic physical and chemical properties in its natural
habitat. However, one such area where the anthropogenic influence is relatively negligible is over the Southern Ocean. Using
115   a combination of data from the active aerosol lidar in space and reanalysis, this study therefore investigates aerosol properties
over the Southern Ocean in relation to the local meteorology. We chose the SH winter period over the Southern Ocean when
solar radiation is at its minimum and DMS emissions are negligible. This is also to make sure that we are predominantly dealing
with sea salt aerosols without contamination via long range transport or local sources. With the advancements in active lidar
remote sensing, it is now feasible to study the optical properties of sea salt aerosols in much detail in their natural environment
120   over larger spatial scales.

In particular, the answers to the following questions are sought.

1. How sensitive are the backscatter, extinction and depolarization ratio to the surface wind speed, relative humidity and the
sea surface temperatures?

2. How is the vertical distribution of aerosol properties impacted by the relative humidity?

125   3. Do the aerosol properties differ during the cyclonic and anticyclonic conditions?

This study would help understand how deliquescent sea salt aerosols are under varying humidities and how the optical
properties of the sea salt aerosols differ at the different stages of the growth.

2 Data and methods

We use a combination of satellite based observations and reanalysis data for the June, July and August months, i.e. southern hemispheric winter, and for the 10-year period (2007-2016) for the investigations. The study area is the latitude band between 40S and 65S. The Cloud-Aerosol Lidar and Infrared Pathfinder Satellite Observations (CALIPSO) Level 2, 5 km Standard Aerosol Profile product (Version 4.20) is used to obtain information on the aerosol properties and their verticality (Winker et al., 2009, 2013), while ERA5 reanalysis is used to get information on humidity and surface winds (Hersbach et al., 2020). We further use geopotential height information at 700 hPa from Atmospheric Infrared Sounder (AIRS) on the Aqua satellites, which flies in the same orbital track as that of CALIPSO, closely in time in the A-Train constellation of satellites. The algorithm theoretical basis document for the most recent Version 7 Level 2 and Level 3 products can be found here: https://docserver.gesdisc.eosdis.nasa.gov/public/project/AIRS/L2_ATBD.pdf We further use the daily sea-ice concentration information from the EUMETSAT's Satellite Application Facility for Ocean and Sea-Ice (OSISAF, 2017).

The quality control and selection of CALIOP data are done as mentioned in the table below.

Parameter/Variable	Selection criteria/condition
Cloud-aerosol discrimination (CAD) score	CAD>= -100 and CAD<=-20
Extinction quality flag	0 (successful retrieval and no change in the initial lidar ratio)
Tropospheric AOD	<= 3.0
Land/Ocean	Only open ocean, sea-ice free profiles and at least 50 km away from the ice-edge
Height	> 500 hPa, lower tropospheric aerosols
Ascending/Descending orbital tracks	Only descending, nighttime

The rationale behind these criteria is as follows. The CAD score between (and equal to) -100 and -20 makes sure that the aerosols are identified with relatively high confidence. The extinction quality flag of 0 ensures that the retrieval converges successfully and there is no need to change the initial lidar ratio. We also investigated additional cases with extinction quality flags of 1 and 2, wherein the lidar ratio was adjusted, but their contribution was little and did not make much difference to the overall statistics presented here. Since the focus here is primarily on sea-salt aerosols, we investigate profiles only over the free open ocean waters and analysed only lower tropospheric aerosols (pressure > 500 hPa), mainly to avoid upper tropospheric aerosols that may be present due to the long-range from the nearby land regions. The profiles over the sea-ice and within 50 km from the ice-edge are removed to avoid potential contamination and misclassification due to the wind-blown snow/ice crystals. We use only nighttime profiles from the descending CALIPSO tracks in order to avoid potential artifacts arising from poorer signal-to-noise ratio during daytime and because we are analysing small changes in the depolarization. The aerosols under the all-sky conditions are analysed here.

Since the parameterizations of the sea salt flux to the atmosphere is primarily a function of three meteorological parameters such as surface wind speed, atmospheric relative humidity and the sea surface temperature (SST), in this study, the extinction, backscatter and depolarization ratio at 532 nm of the marine aerosols are investigated in relation to these meteorological

parameters. During winter months, the Southern Annular Mode (Antarctic Oscillation) plays an important role in driving mete-
155   orological variability in the southern high latitudes. The impact of these phases and the strengths of SAM can be geographical
heterogeneous. When investigating the impact of SAM on aerosol properties, compiling statistics over the entire study area
(40S-65S) could therefore be either misleading or could dampen the potential signal (due to the presence of pockets of low
and high pressure zones over the Southern Ocean). The signal of SAM is visible in the 700 hPa geopotential heights (GPH).
We therefore computed the 25th and 75th percentile thresholds of GPH at each 1x1 degree grid and used them to test if the
160   aerosol properties respond to the two very different regimes, i.e. when the cyclonic and anticyclonic conditions prevail locally.
We compiled and investigated the joint histograms of aerosol properties, mentioned above, when a) the GPH is less than 25th
percentile for cyclonic state and b) the GPH is greater than 75th percentile for anticyclonic state, signalling these two opposite
regimes. In other words, cyclonic and anticyclonic conditions are respectively associated with the ascending and descending
air masses.

3   Results and discussions

3.1   Aerosol properties in relation to wind speed and relative humidity

The 2D joint histograms of total aerosol backscatter at 532 nm as a function of surface wind speed and relative humidity are
presented in Fig. 1 for three atmospheric states - mean state (Clim) (a) and when ascending (P25) (b) and descending (P75) (c)
air masses are encountered. Backscattering coefficient depends both on the number density and on the size of the particles, as
170   well as on refractive index and shape of the particles.

A clear demarcation in the aerosol backscatter at RH ~60% can be seen irrespective of the state of the atmosphere above
which the backscatter increases. This is mainly because of the water uptake by the wind driven sea salt aerosols at high RH
near the ocean surface resulting in an increase in size. An increase in both the number concentration and the mean size of sea
salt aerosols at higher surface wind speeds contribute to an increase in aerosol backscatter for wind speeds stronger than 14
175   m/s. For a drier atmosphere (when RH < 60%), the dependency of backscatter on wind speed is negligible. A plausible reason
is that RH < 60% is mainly encountered at higher altitudes, at which the wind speed does not impact the emission of marine
aerosol. By contrast, higher values of RH are found near the ocean surface, where wind speed directly impacts the size and
number density of emitted particles, thus the backscattering coefficient.

When comparing the ascending (P25) and descending (P75) air masses, an increase in aerosol backscatter is observed in
180   descending air masses for high RH values. This is expected as the large-scale descent inhibits vertical mixing in the atmospheric
column thereby resulting in aerosols being confined to the boundary layer and their proximity to the ocean surface facilitates
the growth of the particles. This is seen more clearly in Fig. 1(d) where the aerosol backscatter is expressed in terms of wind
speed averaged over our study area. The mean state given by the blue curve is very similar to when cyclonic conditions prevail
(red curve). This is because the mean state is dominated by such weather systems during the SH winter months. At low and
185   moderate wind speeds, all three curves are similar (i.e. Clim, P25 and P75). However, at higher wind speeds, elevated aerosol
backscatter is observed during anticyclonic conditions or when descending air masses are encountered. This is because under

such conditions emitted aerosols often remain close to the surface, where the air tends to be more humid, so that the aerosols remain moist. During cyclonic conditions, aerosols in ascending air masses are more frequently exposed to drier air, resulting in evaporation and shrinking of the particles, which reduces the backscattering coefficient.
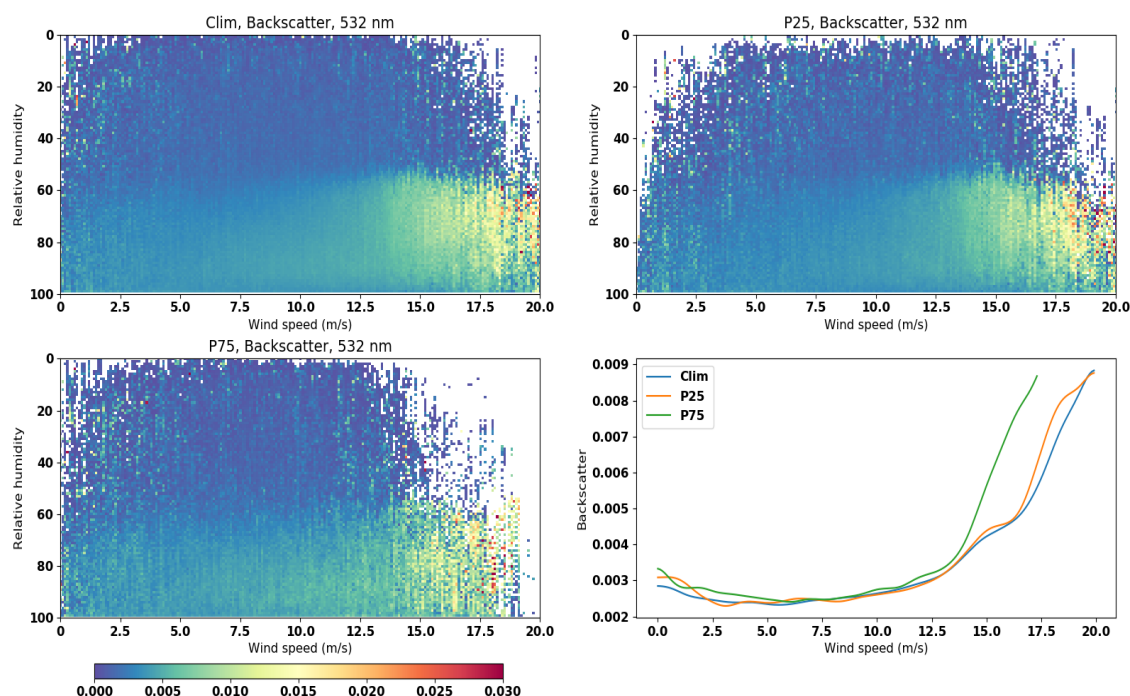
Figure 1. Total backscatter coefficient at 532 nm ($km^{-1}Sr^{-1}$) as a function of surface wind speed and relative humidity. a) Climatological conditions (Clim), all aerosol profiles included, b) only when 700 hPa geopotential height is less than 25%ile (P25) and c) only when 700 hPa geopotential height is greater than than 75%ile (P75). d) Expressed only as a function of wind speed (averaged over all relative humidities).

190   The aerosol extinction for the aforementioned three weather states are shown in Fig. 2. Aerosol extinction is a measure of attenuation of light by absorption and scattering. Similar features as in the aerosol backscattering are observed here also. At higher wind speeds, the extinction increases in a moist atmosphere (RH > 60%) which is indicative of more particles in the atmosphere and large-sized particles which go hand in hand with increased backscattering coefficients. Similar conclusions as in Fig1 can be derived from the curves where the aerosol extinction is expressed in terms of wind speed.

195   The observed distribution of linear depolarization at 532 nm as a function of wind speed and relative humidity is shown in Fig. 3. As seen in aerosol extinction and backscatter parameters, a clear distinction at RH ~60% is observed here too. At low RH, for RH less than 60%, the linear depolarization values are clearly higher indicating a dominance of more non-spherical sea salt particles. Remarkably enough, the linear depolarization is not sensitive to varying winds. The high depolarization cases are more likely from the free troposphere which are decoupled from the surface. It is also evident that there are more non-spherical
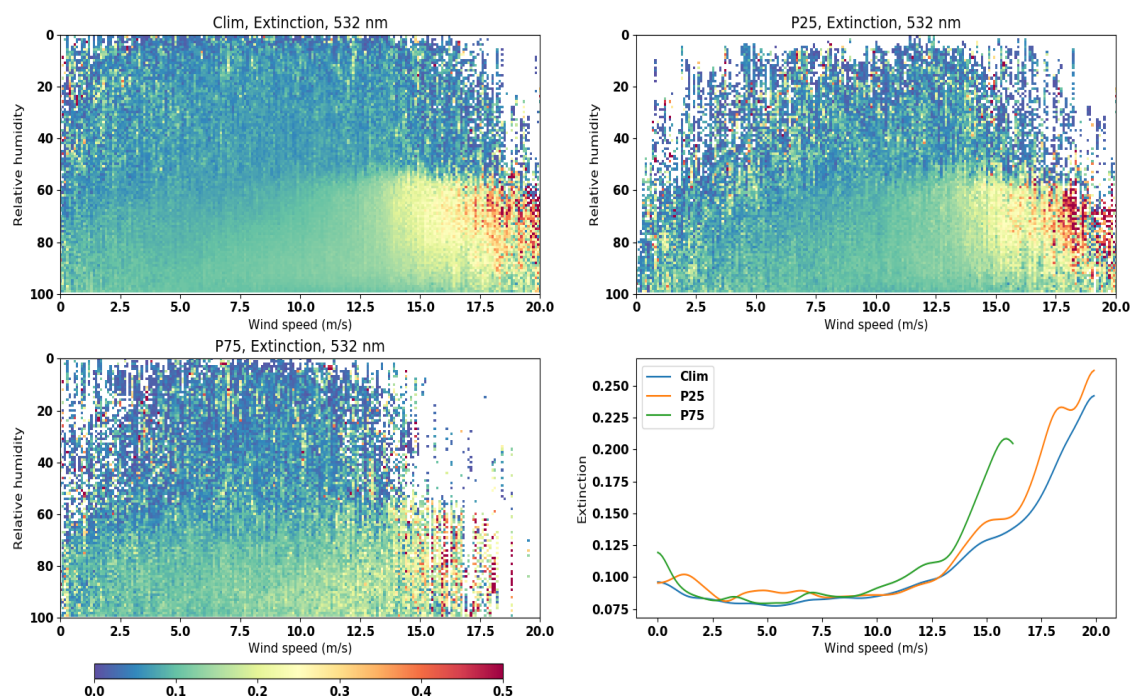
Figure 2. Same as in Fig. 1, but for the extinction coefficient (532 nm).

200 particles when cyclonic conditions prevail compared to the climatological mean state and anticyclonic conditions. This is as expected since the aerosol particles tend to dry out in ascending air parcels as the RH decreases with height. As the RH increases (RH > 60%), water uptake by hydrophilic sea salt particles and subsequent rounding results in lower depolarization values as can be seen in all the three cases. Lab and in-situ measurements have shown that the efflorescence (crystallization) of sea salt occurs at a range of 46-58% RH (Zeng et al., 2013) and deliquescence (the onset of water absorption) occurs at RH

205 around 70-75% (Tang, 1997; Zieger et al., 2017) when the particle starts losing its crystalline structure and tends to be more spherical resulting in lower depolarization values. These RH numbers seem to agree well with what is seen over the Southern Oceans.

   The dependency of linear depolarization on wind speed when the air parcel is classified as 'wet' (solid lines) and 'dry' (dashed lines) conditions based on relative humidity being above and below 60% respectively is shown in Fig. 3(d). This is

210 shown for all three weather states. It is evident that the linear depolarization ratio is significantly higher in dry air masses, indicating the presence of more non-spherical particles compared to moist environments where the particles have a more spherical shape due to water absorption. Also, lower depolarization ratios are observed in ascending air masses compared to descending air masses due to the fact that RH decreases as we move away from the surface. Over the Southern Oceans, inversions in RH were not detected. A slight increase in depolarization ratios with wind speed is noticeable in moist environments.
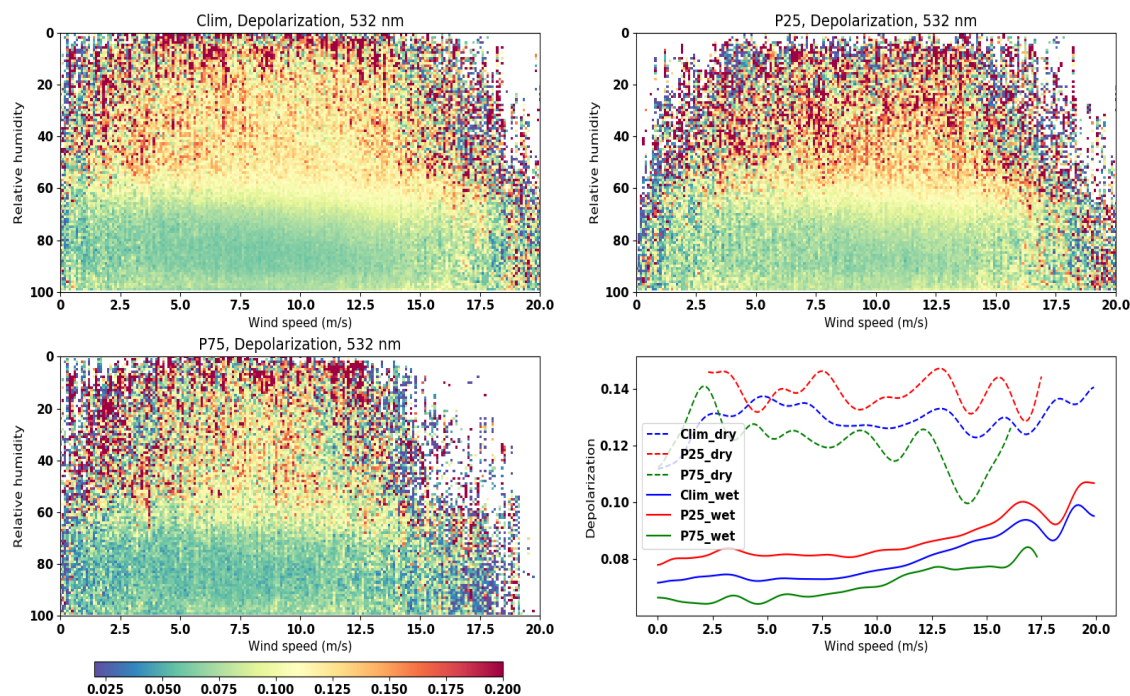
Figure 3. Same as in Fig. 1, but for the particulate depolarization ratio (532 nm). In d) depolarization is further classified in two categories based on the relative humidity, namely dry (RH < 60%) shown as dashed lines and wet (RH > 60%), shown as solid lines and expressed as a function of surface wind speed.

3.2 Aerosol properties in relation to sea surface temperatures

215

Marine aerosol concentration in the atmosphere may also depend indirectly on the temperature by facilitating the evaporation of the sea salt bubbles, if the bubbles are small in size or by accelerating the bursting process with an increase in temperature. Studies have shown that the nano-sized particle concentration decreases with increasing sea water temperature and for particle sizes greater than 0.1 μm, the particle concentration increases with increasing sea water temperature (Nilsson et al., 2007;

220 Martensson et al., 2003). Here, we analyze the optical properties of the marine aerosols over the Southern oceans in relation to wind speed and sea surface temperature. The 532 nm aerosol backscatter and linear depolarization ratio are shown in Fig. 4 and Fig. 5 respectively for the three weather states. In this case, we investigated only the three lowermost quality controlled aerosol profile bins nearest to the surface as they are expected to be influenced most by the SST driven emissions. In the upper layers of the atmosphere, the SST is unlikely to have a direct influence on the backscatter and extinction.

225 Increased aerosol backscatter is observed at higher wind speeds in the climatological mean state and when cyclonic conditions are encountered. However, a dependency on the SSTs is very weak for lower wind speeds in all three weather states. At wind speeds exceeding about 12 m/s, we observe that the backscattering coefficient generally increases with SST. This is
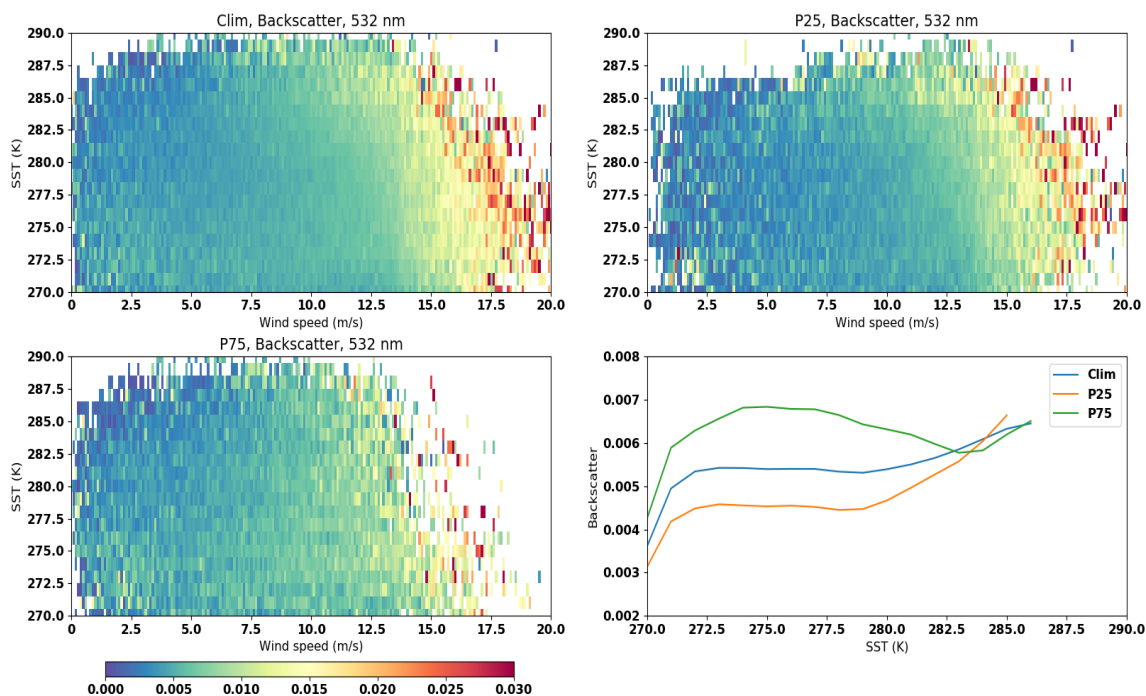
Figure 4. Total backscatter coefficient at 532 nm ($km^{-1}Sr^{-1}$) as a function of surface wind speed and temperature. a) Climatological conditions, all aerosol profiles included, b) only when 700 hPa geopotential height is less than 25%ile (P25), c) only when 700 hPa geopotential height is greater than than 75%ile (P75). d) Expressed only as a function of temperature (averaged over all wind speeds.

consistent with increasing emissions of marine aerosols with increasing SST, as reported in Nilsson et al. (2007); Martensson et al. (2003). When averaged over all wind speeds, the initial 2.5 deg increment (from 270 K to 273 K) in the SST increases the

230 aerosol backscatter coefficient by 30 - 40%, but remains a constant for warm SSTs (i.e. above 273 K). Similar features are also seen in the linear depolarization ratio (Fig. 5). The values increase when temperatures rise from 270 to 273 K and thereafter plateaus until 280 K. However, a slight increase in backscatter and a decrease in depolarization is observed for the SSTs greater than 283 K.

3.3 Verticality of aerosol properties in relation to relative humidity

235 The vertical distribution of backscatter coefficient as a function of RH is presented in Fig.6 for climatological mean state and in ascending (P25) and descending (P75) air masses. In the case of P25 conditions, there are not many observations where RH is lower than 40% in the lowermost troposphere as expected. Aerosol backscatter values in the free troposphere are much lower than in the boundary layer, irrespective of the RH and the three weather states. This indicates that local emissions from the ocean surface make the dominant contribution to aerosol loads over the Southern Ocean. We also see a pronounced dependence
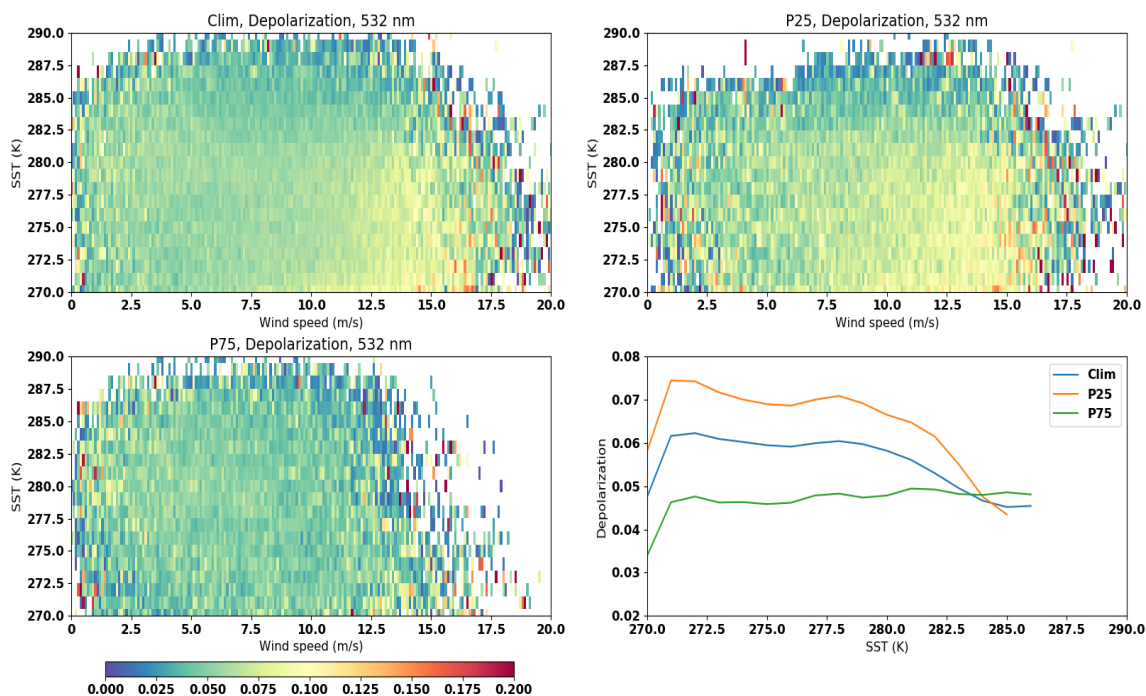
Figure 5. Same as Fig.4, but, for the total linear depolarization ratio (532 nm) as a function of surface wind speed and temperature.

240 of backscattering on RH up to 850 hPa. Elevated values of RH entail a higher aerosol water content, hence larger mean aerosol radius, which results in higher values of the backscattering coefficient. This effect is very pronounced up to 850 hPa. In the free troposphere, no clear dependence of backscattering on RH can be seen. It is possible that the long-range transported aerosols above 850 hPa consists of a mixture of different aerosol species with varying water-adsorption properties. But most importantly, the aerosol in the free troposphere is too tenuous, and the detected signal is too weak to discern a clear relation

245 between RH and backscattering. It is also notable that for any fixed value of RH > 50%, the aerosol layer near the surface has a higher vertical extent during cyclonic conditions (P25) than during anticyclonic conditions (P75), which is what we already mentioned in the discussion of Fig.1. During cyclonic conditions, the lower atmospheric layers are significantly wetter which increases the backscattering coefficients for reasons mentioned above.

The behaviour of backscattering coefficients with RH in the free troposphere (above 850 hPa) and in the lower troposphere

250 are shown in Fig.6d. While there is only a gradual monotonous increase in the backscattering values relative to RH in the free troposphere, a significant increase is observed in the lower troposphere for relative humidities above 40 %. This is, again, an indication that the free troposphere may contain aerosols other than sea salt, which respond differently to changes in RH, while the lower troposphere is likely to be completely dominated by marine aerosol. Note that in the P25 case, there are very few observations available below 850 hPa where RHs are lower than 60% leading to an artifact where there is a sudden increase
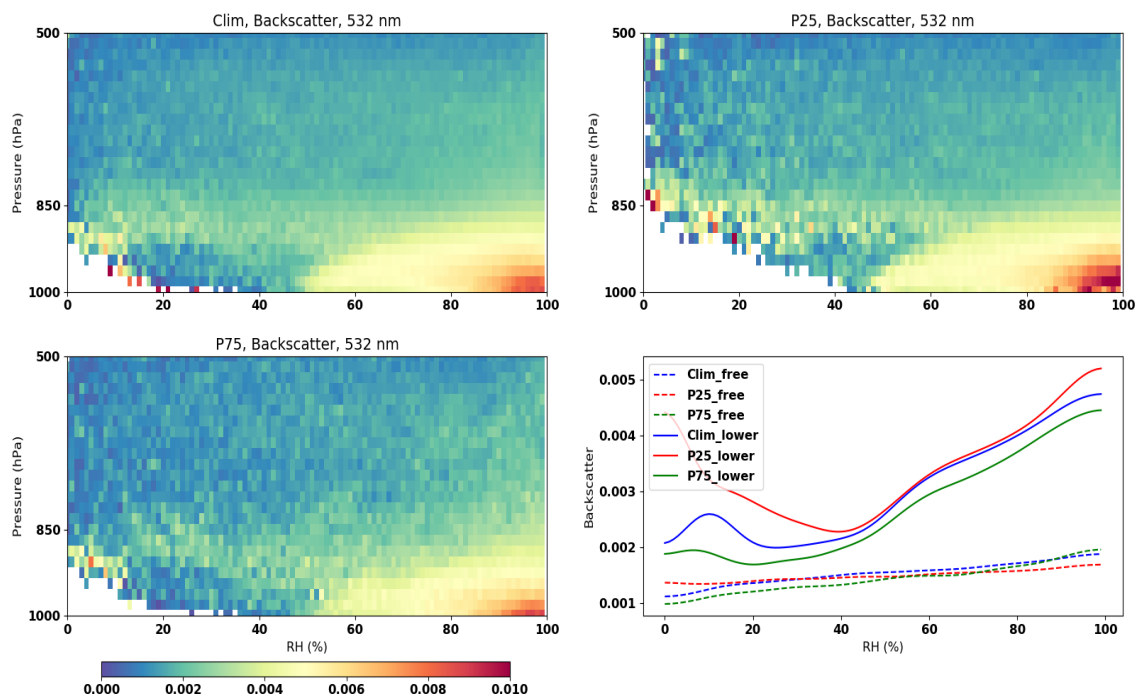
Figure 6. The vertical structure of the total backscatter coefficient at 532 nm (km^{-1}Sr^{-1}) as a function of relative humidity. a) Climatological conditions, all aerosol profiles included, b) only when 700 hPa geopotential height is less than 25%ile (P25), c) only when 700 hPa geopotential height is greater than than 75%ile (P75), d) Expressed only as a function of relative humidity for two cases; the free tropospheric aerosols (pressure < 850 hPa) and the lower tropospheric aerosols (pressure > 850 hPa).

in backscatter at the lower end. We focus now on the lower troposphere (solid lines) and values of RH > 50%. At any given value of RH, we observe higher backscattering values for cyclonic (P25) than for anticyclonic conditions (P75). One possible explanation would be that elevated wind speeds with high aerosol emissions are more prevalent during cyclonic conditions.

The variability of aerosol extinction in the vertical in relation to RH evaluated as joint histograms is shown in Fig.7. All the three weather states show similar features with varying magnitude. We clearly see two maxima in aerosol extinction - in the lower troposphere and in the upper troposphere and the intensity of attenuation increases with increasing RH, more steeply in the lower troposphere. This indicates that the aerosol layer in the free troposphere has different hygroscopicity properties, which can be interpreted as another indication for the presence of long-range transported aerosols aloft that also contain aerosol species other than sea salt. This is further corroborated by the fact that the presence of aerosols in the free troposphere is evident in the extinction profiles, but not in the backscattering profiles. This indicates that the aerosols in the free troposphere may be more strongly absorbing than typical marine aerosols. The increase in extinction with RH seen in the lower troposphere is similar to what is observed in aerosol backscatter. The sharp increase in attenuation occurs at 50 % RH and is associated with

the presence of large aerosol particles. As expected, the extinction coefficient values are slightly less in descending air masses compared to the cyclonic cases.

270 The extinction curves for varying relative humidities when partitioned into lower and free troposphere cases for the three weather states is shown in Fig.7d. In the lower troposphere a steady increase in extinction and a sharp increase beyond 50% RH is observed in all the cases. Extinction by marine aerosols is dominated by scattering. Thus, the extinction curves in the lower troposphere display a dependence on RH that is very similar to that of the backscattering curves in Fig. 6d. In the upper troposphere, the dependence of extinction on RH is much weaker, which we attribute to the presence of other, presumably less hygroscopic aerosol species. By contrast to the lower troposphere, the aerosol extinction is higher in the P75 case compared to 275 the other two states in the free troposphere.
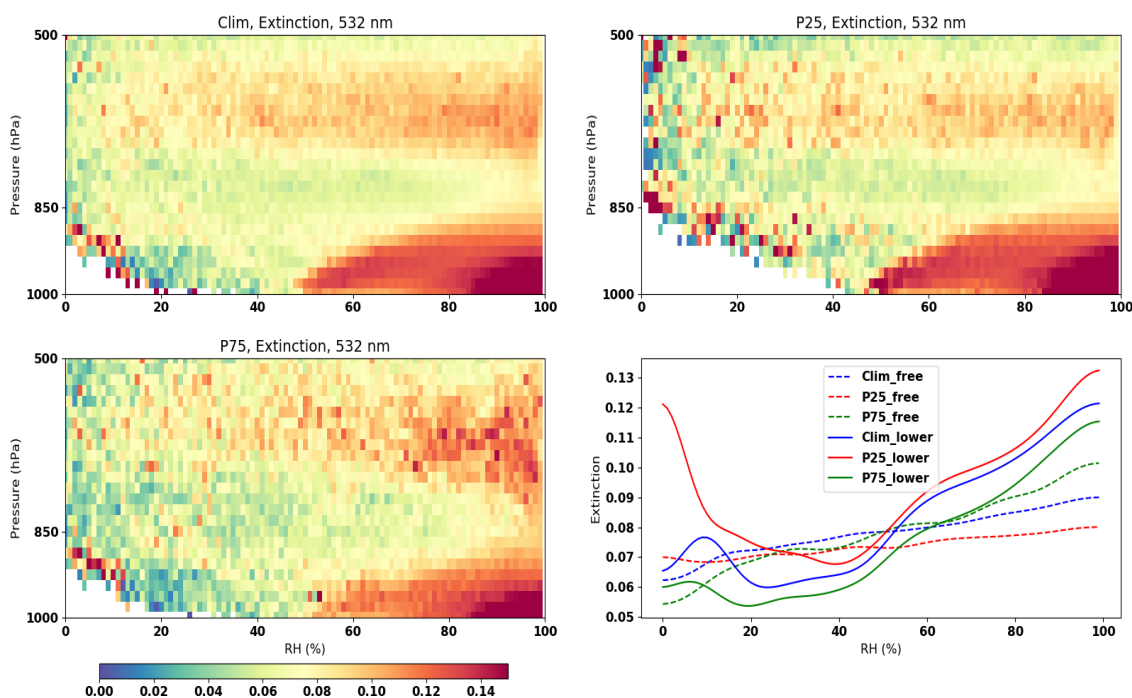
Figure 7. Same as in Fig. 6, but for the extinction coefficient (532 nm).

While backscatter coefficient and extinction coefficient are indicative of the presence of aerosols and their size, linear depolarization ratio gives information about the morphology of the aerosols, i.e. if the particles are spherical or nonspherical. Dry sea salt particles have shapes similar to cubes, which can have depolarisation ratios up to, but rarely exceeding 0.20 (see Kanngießer and Kahnert (2021), and references therein). As more water is adsorbed, the particles become more spherical, and 280 the salt core is partially or completely dissolved in the liquid coating. The depolarisation ratio of homogeneous spheres is

identically zero. Thus the depolarisation ratio should anti-correlate to the water content of the particles, which, in turn, depends on RH.

As seen in the earlier section, RH is one of the major factors that can impact the depolarization ratio of a particle. Here, we analyze the vertical distribution of this ratio as a function of RH for the three weather states (Fig.8). A clear separation is

285 observed in the free and lower troposphere, more prominent in the climatological mean and the cyclonic states. For RH > 60%, low depolarisation values are noticeable in the lower troposphere, which is an indication of the dominance of water-coated, mostly spherical sea salt particles. For RH < 60%, there are instances when the aerosol depolarization increases in the boundary layer, more prominently in the mean and anticyclonic cases which can be associated with the presence of drier aerosol particles.
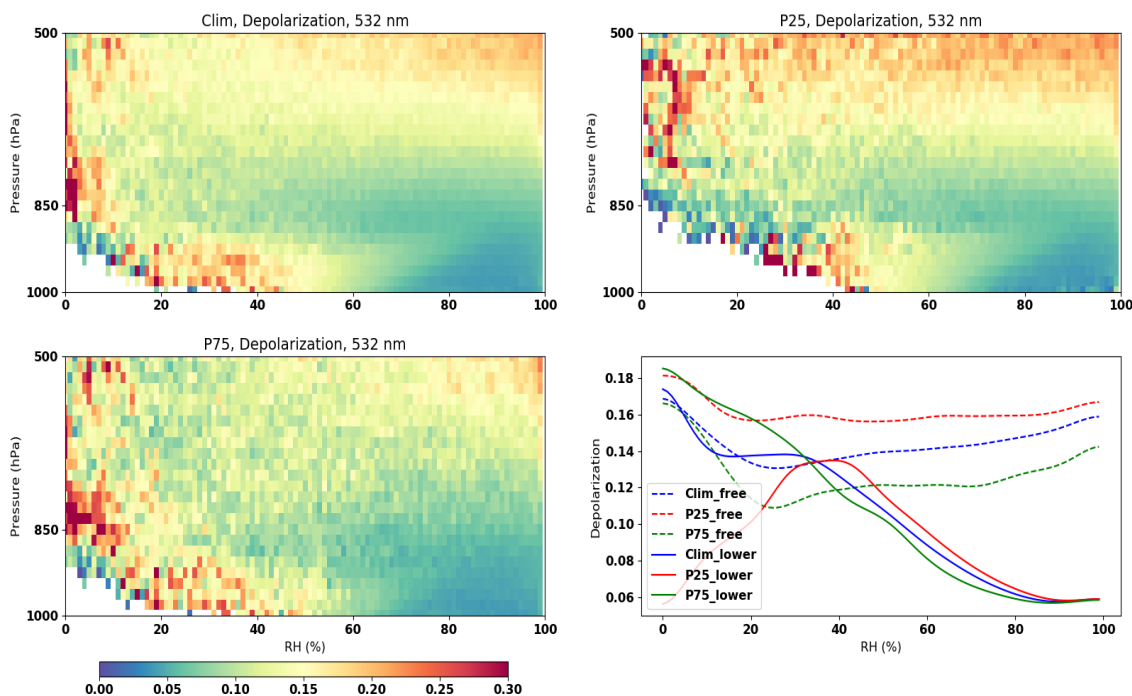
Figure 8. Same as in Fig.6, but for the particulate depolarization ratio (532 nm).

As seen by comparison with Fig. 7, the region of high values of aerosol extinction in the upper troposphere coincides with

290 high depolarization values irrespective of the RH values. Again, this indicates the presence of long-range transported aerosols of mixed composition, which evidently have water adsorption properties different from those of pure marine aerosols. However, the composition of these aerosols is unknown, and it may, indeed, be highly variable in space and time. It is, therefore, much more difficult to interpret this data. Fig. 8d shows the depolarisation ratio as a function of RH, averaged over the geographic domain and the study period. . High depolarization values at the lower end of the RH spectrum indicate the presence of non-

295 spherical particles. For 40% < RH < 100% the depolarisation in the lower troposphere is characterised by a steep but gradual

decrease with increasing RH. This is true for all three weather states. However, we do not see any sudden changes in the depolarisation ratio. One may have expected such changes at the efflorescence point or at the deliquescence point, at which pure sodium chloride could undergo rapid changes in water content, hence in shape. We can conclude that the decrease of the depolarisation ratio with increasing RH in the lower troposphere is consistent with a change in sea salt morphology from

300   nonspherical to spherical shape, which is caused by increased water adsorption with growing RH. However, our averaged data set does not display any evidence of sudden crystallisation, deliquescence, or hysteresis effects in water content. This does not rule out the existence of such effects; but discovering them will likely require a targeted investigation of individual cases, rather than an analysis of temporally and geographically averaged large data sets. We note that for RH < 35% the P25-curve diverges from the climatological and the P75-curve. However, such low RH-values during cyclonic conditions are rather rare. Thus, this

305   part of the curve is based on fairly sparse data and may well be an artifact.
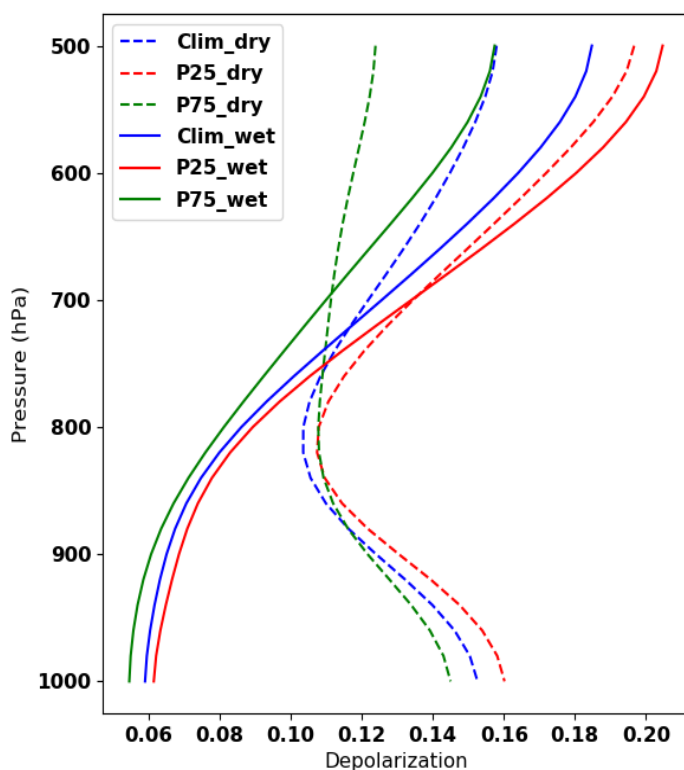
Figure 9. The vertical structure of depolarization ratio for two relative humidity groups; when relative humidities are between 20% to 60% (drier conditions, dashed lines) and when they are between 60% - 100% (wetter conditions, solid lines). The three colours show climatological, P25 and P75 conditions.

In Fig.9, the vertical distribution of depolarization ratios is analyzed for two ranges of relative humidities that characterizes drier and wetter atmospheric conditions over the Southern Oceans. The RH range between 20 and 60% is considered as 'dry' and when RH exceeds 60%, those air parcels are considered 'wet'. The three curves show the three weather states. It can be clearly seen that the drier air masses always have substantially higher depolarization ratios in the lower atmospheric levels than

310 the moist aerosols. However, this ratio decreases with height until 800 hPa and then increases. This behaviour can also be seen in the colour panels in Fig. 8. As mentioned earlier, we have two distinct aerosol layers, one marine aerosol layer near the surface and one mixed layer in the free troposphere. The region around 800 hPa marks the boundary between these layers that is characterised by low aerosol concentrations, which explains the minimum in the depolarisation curve under dry conditions. By contrast, owing to the predominance of spherical shape, the wet aerosols have a low depolarization ratio, despite their high

315 concentration near the surface. Irrespective of the weather state the ratio increases with height indicating more non-spherical aerosols due to lack of moisture resulting from a decrease of RH in the vertical. The wet aerosols encountered during cyclonic conditions have higher depolarization ratios compared to those encountered during anticyclonic conditions. Again, above 800 hPa, where we expect to find long-range transported mixed aerosol populations, the interpretation of the depolarisation ratio and its dependence on the vertical coordinate and RH is rather elusive.

320 **4 Conclusions**

70% of the Earth's area is covered by water. The marine aerosols, especially sea salt, are therefore one of the dominant sources of the total aerosol load in the atmosphere. The significant climate implications of marine aerosols call for better understanding of their variability and coupling with the local meteorological conditions. The Southern Ocean is unique in this context, as the boundary layer is relatively free from the influence of anthropogenic aerosols and dust (compared to the northern hemispheric

325 oceans). During the southern hemispheric wintertime the influence of natural DMS emissions on the total aerosol load is also negligible over the Southern Ocean, allowing investigations of sea salt aerosols. Using 10 years of wintertime (June, July and August, 2007-2016) space based profiling of aerosols by CALIOP-CALIPSO in combination with meteorological reanalysis data, we investigated the sensitivity of marine aerosol properties over the Southern Ocean to various meteorological parameters, such as relative humidity, near surface wind speed, and sea surface temperature in terms of joint histograms. The sensitivity

330 study is done for the climatological conditions as well as during the enhanced cyclonic (P25) and anticyclonic conditions (P75) in order to understand the impact of large-scale atmospheric circulation on the aerosol properties. These conditions were defined based on the 700 hPa geopotential height being either below 25%ile (P25, cyclonic, ascending air masses) or above 75%ile (P75, anticyclonic, descending air masses).

The following conclusions are drawn based on this sensitivity analysis.

335

a) A clear demarcation in the 532 nm aerosol backscatter and extinction at RH ~60% can be seen irrespective of the state of the atmosphere. The backscatter and extinction increase at higher relative humidity as a function of wind speed. This is mainly because of the water uptake by the wind driven sea salt aerosols at high RH near the ocean surface resulting in an increase in

size, which is confirmed by the decreased depolarization for the wet aerosols.

340

b) An increase in aerosol backscatter and extinction is observed during the anticyclonic conditions compared to cyclonic conditions for the higher wind speeds and relative humidity, mainly due to aerosols being confined to the boundary layer and their proximity to the ocean surface facilitates the growth of the particles.

345   c) At lower wind speeds, there is a very weak dependency of aerosol backscatter on the SSTs. At wind speeds exceeding about 12 m/s, the backscattering coefficient generally increases with SST.

d) When aerosol properties are investigated in terms of aerosol verticality and in relation to meteorological parameters, it is seen that the aerosol backscatter values in the free troposphere (pressure < 850 hPa) are much lower than in the boundary
350   layer, irrespective of the RH and the three weather states. This indicates that the local emissions from the ocean surface make the dominant contribution to aerosol loads over the Southern Ocean.

e) We see a pronounced dependence of backscattering on RH up to 850 hPa. Elevated values of RH entail a higher aerosol water content, hence larger mean aerosol radius, which results in higher values of the backscattering coefficient. This effect is
355   very pronounced up to 850 hPa. In the free troposphere, no clear dependency of backscattering on RH can be seen.

f) A clear separation of linear depolarization is observed in the free and lower troposphere, more prominent in the climatological mean and the cyclonic states. For RH > 60%, low depolarization values are noticeable in the lower troposphere, which is an indication of the dominance of water-coated, mostly spherical sea salt particles. For RH < 60%, there are instances when
360   the aerosol depolarization increases in the boundary layer, more prominently in the mean and anticyclonic cases which can be associated with the presence of drier aerosol particles. Under very dry conditions, the depolarisation ratio of marine aerosols in the boundary layer can be as high as 0.16.

g) Interpreting the verticality of aerosol properties (especially depolarization) in relation to the meteorological conditions
365   in the free and upper troposphere (pressure < 850 hPa) is however difficult and challenging in a statistical sense. The tracer transport studies are required to assess the contribution and mixing of anthropogenic and natural biomass burning pollutants in the free troposphere.

Data availability.

All data sets used here are publicly available. The links to the data sets are given below:
370   https://asdc.larc.nasa.gov/project/CALIPSO/CAL_LID_L2_05kmAPro-Standard-V4-20_V4-20
https://www.ecmwf.int/en/forecasts/dataset/ecmwf-reanalysis-v5

Author contributions.

MT carried out the analysis and wrote the first draft of the manuscript. All authors contributed to the design of experiments, interpretation of the results and writing.

375 *Competing interests.* The authors declare no competing interests.

Acknowledgements. The authors acknowledge the funding from Swedish National Space Agency (Project nr. 126/19) for this study.

References

Andreas, E. L.: A new sea spray generation function for wind speeds up to 32 m/s, J. Phys. Oceanogr., p. 2175–2184, 1998.

Bates, T. S., Huebert, B. J., Gras, J. L., Griffiths, F. B., and Durkee, P. A.: International Global Atmospheric Chemistry (IGAC) Project's First Aerosol Characterization Experiment (ACE 1): Overview, J. Geophys. Res., pp. 16,297– 16,318, https://doi.org/10.1029/97JD03741, 1998a.

Clarke, A. D., Owens, S. R., and Zhou, J.: An ultrafine sea-salt flux from breaking waves: Implications for cloud condensation nuclei in the remote marine atmosphere, J. Geophys. Res-Atmos., 111, https://doi.org/10.1029/2005JD006565, 2006.

Cotterell, M. I., Willoughby, R. E., Bzdek, B. R., Orr-Ewing, A. I., and Reid, J. P.: A complete parameterization of the relative humidity and wavelength dependence of the refractive index of hygroscopic inorganic aerosol particles, Atmospheric Chemistry and Physics,, p. 9837–9851, https://doi.org/10.5194/acp-17-9837-2017, 2017.

de Leeuw, G., Neele, F. P., Hill, M., Smith, M. H., and Vignati, E.: Production of sea spray aerosol in the surf zone, J. Geophys. Res., p. 29397–29409, https://doi.org/10.1029/2000JD900549, 2000.

Froyd, K. D., Murphy, D. M., Brock, C. A., Campuzano-Jost, P., Dibb, J. E., Jimenez, J.-L., Kupc, A., Middlebrook, A. M., Schill, G. P., Thornhill, K. L., Williamson, C. J., Wilson, J. C., and Ziemba, L. D.: A new method to quantify mineral dust and other aerosol species from aircraft platforms using single particle mass spectrometry, Atmos. Meas. Tech., https://doi.org/10.5194/amt-12-6209-2019, 2019.

Fuelberg, H. E., Newell, R. E.and Westberg, D. J., Maloney, J. C., Hannan, J. R., Martin, B. D., Avery, M. A., and Zhu, Y.: A meteorological overview of the second Pacific Exploratory Mission in the tropics, J. Geophys. Res., https://doi.org/10.1029/2001JD900173, 2001.

Gong, S. L.: A parameterization of sea-salt aerosol source function for sub- and super-micron particles, Global Biogeochem. Cycles, p. 1097, https://doi.org/10.1029/2003GB002079, 2003.

Grythe, H., Ström, J., Krejci, R., Quinn, P., and Stohl, A.: A review of sea-spray aerosol source functions using a large global set of sea salt aerosol concentration measurements, Atmos. Chem. Phys., p. 1277–1297, https://doi.org/10.5194/acp-14-1277-2014, 2014.

Guelle, W., Schulz, M., Balkanski, Y., and Dentener, F.: Influence of the source formulation on modeling atmospheric global distribution of sea salt aerosol, J. Geophys. Res., p. 27509–27524, https://doi.org/10.1029/2001JD900249, 2001.

Haarig, M., Ansmann, A., Althausen, D., Klepel, A., Groß, S., Freudenthaler, V., Toledano, C., Mamouri, R.-E., Farrell, D. A., Prescod, D. A., Marinou, E., Burton, S. P., Gasteiger, J., Engelmann, R., and Baars, H.: Triple-wavelength depolarization-ratio profiling of Saharan dust over Barbados during SALTRACE in 2013 and 2014, Atmos. Chem. Phys., p. 10767–10794, https://doi.org/10.5194/acp-17-10767-2017, 2017.

Haywood, J. M., Ramaswamy, V., and Soden, B. J.: Tropospheric Aerosol Climate Forcing in Clear-Sky Satellite Observations over the Oceans., Science, p. 1299–1303, https://doi.org/10.1126/science.283.5406.1299, 1999.

Hersbach, H., Bell, B., Berrisford, P., Hirahara, S., Horányi, A., Muñoz-Sabater, J., Nicolas, J., Peubey, C., Radu, R., Schepers, D., Simmons, A., Soci, C., Abdalla, S., Abellan, X., Balsamo, G., Bechtold, P., Biavati, G., Bidlot, J., Bonavita, M., De Chiara, G., Dahlgren, P., Dee, D., Diamantakis, M., Dragani, R., Flemming, J., Forbes, R., Fuentes, M., Geer, A., Haimberger, L., Healy, S., Hogan, R. J., Hólm, E., Janisková, M., Keeley, S., Laloyaux, P., Lopez, P., Lupu, C., Radnoti, G., de Rosnay, P., Rozum, I., Vamborg, F., Villaume, S., and Thépaut, J.-N.: The ERA5 global reanalysis., Q. J. R. Meteorol. Soc., p. 1999–2049, https://doi.org/10.1002/qj.3803, 2020.

Irshad, R., Grainger, R. G., Peters, D. M., McPheat, R. A., Smith, K. M., and Thomas, G.: Laboratory measurements of the optical properties of sea salt aerosol, Atmos. Chem. Phys., p. 221–230, https://doi.org/10.5194/acp-9-221-2009, 2009.

Jaeglé, L., Quinn, P. K., Bates, T. S., Alexander, B., and Lin, J.-T.: Global distribution of sea salt aerosols: new constraints from in situ and remote sensing observations, Atmos. Chem. Phys., p. 3137–3157, https://doi.org/10.5194/acp-11-3137-2011, 2011.

415 Kanngießer, F. and Kahnert, M.: Modeling optical properties of non-cubical sea-salt particles, J. Geophys. Res., p. e2020JD033674, https://doi.org/10.1029/2020JD033674, 2021.

Kaufman, Y. J., Smirnov, A., Holben, B. N., and Dubovik, O.: Baseline maritime aerosol: methodology to derive the optical thickness and scattering properties, Geophys. Res. Lett., p. 3251–3254, https://doi.org/10.1029/2001GL013312, 2001.

Lewis, E. R. and Schwartz, S. E.: Sea Salt Aerosol Production: Mechanisms, Methods, Measurements, and Models: A Critical Review,

420 American Geophysical Union, Washington, DC, USA, 2004.

Ma, X., Von Salzen, K., and Li, J.: Modelling sea salt aerosol and its direct and indirect effects on climate, Atmos. Chem. Phys., p. 1311–1327, https://doi.org/10.5194/acp-8-1311-2008, 2008.

Martensson, E., Nilsson, E., Leeuw, G., Cohen, L., and Hansson, H.: Laboratory simulations and parameterization of the primary marine aerosol production, J. Geophys. Res.-Atmos., p. 4297, https://doi.org/10.1029/2002JD002263, 2003.

425 Monahan, E. C., Spiel, D. E., and Davidson, K. L.: A model of marine aerosol generation via whitecaps and wave disruption, in Oceanic Whitecaps, edited by E. Monahan, and G. M. Niocaill, Springer, Dordrecht, pp. 167–174, https://doi.org/10.1007/978-94-009-4668-2_16, 1986.

Murphy, D. M., Froyd, K. D., Bian, H., Brock, C. A., Dibb, J. E., DiGangi, J. P., Diskin, G., Dollner, M., Kupc, A., Scheuer, E. M., Schill, G. P., Weinzierl, B., Williamson, C. J., and Yu, P.: The distribution of sea-salt aerosol in the global troposphere, Atmos. Chem. Phys., p.

430 4093–4104, https://doi.org/10.5194/acp19-4093-2019, 2019.

Neumann, D., Matthias, V., Bieser, J., Aulinger, A., and Quante, M.: A comparison of sea salt emission parameterizations in northwestern Europe using a chemistry transport model setup, Atmos. Chem. Phys., p. 9905–9933, https://doi.org/10.5194/acp-16-9905-2016, 2016.

Nilsson, E. D., Mårtensson, E. M., Van Ekeren, J. S., de Leeuw, G., Moerman, M., and O'Dowd, C.: Primary marine aerosol emissions: size resolved eddy covariance measurements with estimates of the sea salt and organic carbon fractions, Atmos. Chem. Phys. Discuss., p.

435 13345–13400, https://doi.org/10.5194/acpd-7-13345-2007, 2007.

OSISAF(2017): Global Sea Ice Concentration Climate Data Record v2.0 - Multimission, EUMETSAT SAF on Ocean and Sea Ice, https://doi.org/10.15770/EUM_SAF_OSI_0008, 2017.

O'Dowd, C. D., Smith, M. H., Costerdine, I. E., and Lowe, J. A.: Marine aerosol, sea salt, and the marine sulphur cycle: A short review, Atmos. Env., pp. 73–80, https://doi.org/10.1016/S1352-2310(96)00106-9, 1997.

440 Pierce, J. R. and Adams, P. J.: Global evaluation of CCN formation by direct emission of sea salt and growth of ultrafine sea salt, J. Geophys. Res., p. D06203, https://doi.org/10.1029/2005JD006186, 2006.

Revell, L. E., Kremser, S., Hartery, S., Harvey, M., Mulcahy, J. P., Williams, J., Morgenstern, O., McDonald, A. J., Varma, V., Bird, L., and Schuddeboom, A.: The sensitivity of Southern Ocean aerosols and cloud microphysics to sea spray and sulfate aerosol production in the HadGEM3-GA7.1 chemistry–climate model, Atmos. Chem. Phys., p. 15447–15466, https://doi.org/10.5194/acp-19-15447-2019, 2019.

445 Sakai, T., Nagai, T., Zaizen, Y., and Mano, Y.: Backscattering linear depolarization ratio measurements of mineral, sea-salt, and ammonium sulfate particles simulated in a laboratory chamber, Appl. Opt., pp. 4441–4449, https://doi.org/10.1364/AO.49.004441, 2010.

Shindell, D. T., Lamarque, J.-F., Schulz, M., Flanner, M., Jiao, C., Chin, M., Young, P. J., Lee, Y. H., Rotstayn, L., Mahowald, N., Milly, G., Faluvegi, G., Balkanski, Y., Collins, W. J., Conley, A. J., Dalsoren, S., Easter, R., Ghan, S., Horowitz, L., Liu, X., Myhre, G., Nagashima, T., Naik, V., Rumbold, S. T., Skeie, R., Sudo, K., Szopa, S., Takemura, T., Voulgarakis, A., Yoon, J.-H., and Lo, F.: Radiative forcing in the

450 ACCMIP historical and future climate simulations, Atmos. Chem. Phys., p. 2939–2974, https://doi.org/10.5194/acp-13-2939-2013, 2013.

Shinozuka, Y., Clarke, A. D., Howell, S. G., Kapustin, V. N., and Huebert, B. J.: Sea-salt vertical profiles over the Southern and tropical Pacific oceans: Microphysics, optical properties, spatial variability, and variations with wind speed, J. Geophys. Res., p. D24201, https://doi.org/10.1029/2004JD004975, 2004.

Sievering, H., Boatman, J., Gorman, E., Kim, Y., Anderson, L., Ennis, G., Luria, M., and Pandis, S.: Removal of sulfur from the marine boundary layer by ozone oxidation in sea-salt aerosols, Nature, 360, 571–573, https://doi.org/10.1038/360571a0, 1992.

Smith, M. H., Park, P. M., and Consterdine, I. E.: Marine aerosol concentrations and estimated fluxes over sea, Q. J. R. Meteorol. Soc., p. 809–824, https://doi.org/10.1002/qj.49711951211, 1993.

Spada, M., Jorba, O., García-Pando, C. P., Janjic, Z., and Baldasano, J. M.: On the evaluation of global sea-salt aerosol models at coastal/orographic stations, Atmos. Env., pp. 41–48, https://doi.org/10.1016/j.atmosenv.2014.11.019, 2015.

Stevens, B., Farrell, D., Hirsch, L., Jansen, F., Nuijens, L., Serikov, I., Brügmann, B., Forde, M., Linne, H., Lonitz, K., and Prospero, J. M.: he Barbados Cloud Observatory: Anchoring investigations of clouds and circulation on the edge of the ITCZ, Bull. Amer. Meteor. Soc., p. 787–801, https://doi.org/10.1175/BAMS-D-14-00247.1, 2016.

Tang, I. N.: Chemical and size effects of hygroscopic aerosols on light scattering coefficients, J. Geophys. Res., pp. 19,245 – 19,250, https://doi.org/10.1029/96JD03003, 1996.

Tang, I. N.: Thermodynamic and optical properties of sea salt aerosol., J. Geophys. Res., p. 23269–23275, https://doi.org/10.1029/97JD01806, 1997.

Tsyro, S., Aas, W., Soares, J., Sofiev, M., Berge, H., and Spindler, G.: Modelling of sea salt concentrations over Europe: key uncertainties and comparison with observations,, Atmos. Chem. Phys., p. 10367–10388, https://doi.org/10.5194/acp-11-10367-2011, 2011.

Vignati, E., de Leeuw, G., and Berkowicz, R.: Modeling coastal aerosol transport and effects of surf-produced aerosols on process in the marine atmospheric boundary layer, J. Geophys. Res., pp. 20,225–20,238, https://doi.org/10.1029/2000JD000025, 2001.

Vogt, R., Sander, R., von Glasow, R., and Crutzen, P. J.: Iodine Chemistry and its Role in Halogen Activation and Ozone Loss in the Marine Boundary Layer: A Model Study, J. Atmos. Chem., p. 375–395, https://doi.org/10.1023/A:1006179901037, 1999.

Weng, H., Lin, J., Martin, R., Millet, D., Jaeglé, L., Ridley, D., Keller, C., Li, C., Du, M., and Meng, J.: Global high-resolution emissions of soil NOx, sea salt aerosols, and biogenic volatile organic compounds, Scientific Data, p. 148, https://doi.org/10.1038/s41597-020-0488-5, 2020.

Winker, D. M., Vaughan, M. A., Omar, A., Hu, Y., Powell, K. A., Liu, Z., Hunt, W. H., and Young, S. A.: Overview of the CALIPSO Mission and CALIOP Data Processing Algorithms, Journal of Atmospheric and Oceanic Technology, pp. 2310–2323, https://doi.org/10.1175/2009JTECHA1281.1, 2009.

Winker, D. M., Tackett, J. L., Getzewich, B. J., Liu, Z., Vaughan, M. A., and Rogers, R. R.: The global 3-D distribution of tropospheric aerosols as characterized by CALIOP, Atmos. Chem. Phys., p. 3345–3361, https://doi.org/10.5194/acp-13-3345-2013, 2013.

Wise, M. E., Freney, E. J., Tyree, C. A., Allen, J. O., Martin, S. T., Russell, L. M., and Buseck, P. R.: Hygroscopic behavior and liquid-layer composition of aerosol particles generated from natural and artificial seawater, J. Geophys. Res., p. D03201, https://doi.org/10.1029/2008JD010449, 2009.

Zeng, J., Zhang, G., Long, S., Liu, K., Cao, L., Bao, L., and Li, Y.: Sea salt deliquescence and crystallization in atmosphere: An in situ investigation using X-ray phase contrast imaging, Surface and Interface Analysis, p. 930– 936, https://doi.org/10.1002/sia.5184, 2013.

Zhang, K. M., Knipping, E. M., Wexler, A. S., Bhave, P. V., and Tonnesen, G. S.: Size distribution of sea-salt emissions as a function of relative humidity., Atmos. Env., p. 3373– 3379, https://doi.org/10.1029/96JD03003, 2005.

Zhu, L., Jacob, D., Eastham, S. D., Sulprizio, M. P., Wang, X., Sherwen, T., Evans, M., Chen, Q., Alexander, B., Koenig, T., Volkamer, R., Huey, L. G., Breton, M. L., Bannan, T. J., and Percival, C.: Effect of sea salt aerosol on tropospheric bromine chemistry, Atmos. Chem. Phys., p. 6497–6507, https://doi.org/10.5194/acp-19-6497-2019, 2019.

Zieger, P., Fierz-Schmidhauser, R., Weingartner, E., and Baltensperger, U.: Effects of relative humidity on aerosol light scattering: results from different European sites., Atmos. Chem. Phys., p. 10609–10631, https://doi.org/10.5194/acp-13-10609-2013, 2013.

Zieger, P., Väisänen, O., Corbin, J. C., Partridge, D. G., Bastelberger, S., Mousavi-Fard, M., Rosati, B., Gysel, M., Krieger, U., Leck, C., Nenes, A., Riipinen, I., Virtanen, A., and Salter, M. E.: Revising the hygroscopicity of inorganic sea salt particles., Nat. Comm., https://doi.org/10.1038/ncomms15883, 2017.